Journal of Alloys and Compounds 480 (2009) 208–215

Contents lists available at ScienceDirect

Journal of Alloys and Compounds

journal homepage: www.elsevier.com/locate/jallcom

Fluorescence and Judd–Ofelt analysis of Nd^{3+} doped P_2O_5–Na_2O–K_2O glass

G.N. Hemantha Kumar[a], J.L. Rao[b], K. Ravindra Prasad[a], Y.C. Ratnakaram[a,*]

[a] Department of Physics, Sri Venkateswara University P.G. Centre, Kavali-524 201, India
[b] Department of Physics, Sri Venkateswara University, Tirupati-517 502, India

ARTICLE INFO

Article history:
Received 6 December 2008
Received in revised form 5 February 2009
Accepted 10 February 2009
Available online 23 February 2009

Keywords:
Absorption
Fluorescence
Phosphate glass
Lifetime
Cross-section

ABSTRACT

Sodium potassium phosphate glass consisting different Nd_2O_3 concentrations have been prepared to study the effect of Nd^{3+} concentration on optical absorption and fluorescence properties. From the absorption spectra, Racah (E^1, E^2, E^3), spin-orbit (ξ_{4f}) and configuration interaction (α) parameters are calculated and reported for all the Nd^{3+} doped glasses. Judd–Ofelt intensity parameters (Ω_2, Ω_4, Ω_6) are evaluated and these parameters are used to study the covalency as a function of Nd^{3+} concentration. Results show that covalency decreases with the increase of Nd^{3+} concentration. By using these three intensity parameters, total radiative transition probabilities (A_T), radiative lifetimes (τ_R), branching ratios (β) and integrated absorption cross-sections (Σ) have been computed for certain excited states of Nd^{3+} in these mixed alkali phosphate glasses for all the concentrations. From the fluorescence spectra, peak stimulated emission cross-sections (σ_p) have been calculated for the two transitions, $^4G_{7/2} \rightarrow {}^4I_{13/2}$ and $^4G_{7/2} \rightarrow {}^4I_{11/2}$ of Nd^{3+} in all these glass matrices. From the absorption spectra, the optical band gaps (E_{opt}) for both direct and indirect transitions have been obtained. All these spectroscopic parameters are compared for different Nd^{3+} concentrations. From these studies, a few transitions are identified for laser excitation among various transitions.

1. Introduction

Rare earth elements in glasses have been widely studied due to their important applications for optical telecommunications and laser technology [1,2]. The rapid developments in information technology depend on the materials, which are useful for information transmission, power transmission and nonlinear applications. Among various glass matrices, phosphate glass systems are technologically interesting amorphous materials due to their low glass transition temperatures and high thermal expansion coefficients [3]. Phosphate glasses act as good hosts for large concentrations of dopant rare earth ions with good homogeneity. Materials with a range of compositions have been studied with high-resolution solid state NMR and complimentary techniques [4]. Among various rare earth ions neodymium is the most widely investigated ion in a variety of glasses not only because of its potential applications but also because of the variations in its spectroscopic properties with composition. These properties include absorption and emission cross-sections, radiative and non-radiative transition rates and quantum efficiencies.

The 'mixed alkali effect' is a term describing the nonlinear variation in glass properties (such as density, viscosity, glass transition temperature and conductivity) when one alkali in a multicomponent glass is systematically replaced by another species [5–7]. This nonlinear behavior is not limited to glasses containing only alkali ions; certain mixed alkali–alkaline earth oxide glasses display nonlinear trends in physical properties as a function of composition [8]. The mixed alkali phenomenon is useful in manufacturing low loss electrical glass and in understanding chemical strengthening of glass [5]. Green et al. [9] found that the relaxation times that characterize the response of mixed alkali metaphosphate glasses to mechanical and electrical perturbations, τ_μ and τ_σ respectively, are orders of magnitude larger than the relaxation times in single alkali metaphosphate glasses. Earlier, the authors have studied the effect of mixed alkalis on spectroscopic properties of different rare earth ions [10–12]. Most of the researchers used mixed alkalis in the glass, have tried to understand the mixed alkali effect by varying the compositions of alkalis. However, less attention has been paid to understand the local environment of rare earth ions by varying its concentration in a phosphate glass containing mixed alkalis. In the present work, to see the effect of Nd^{3+} concentration on absorption and emission properties, sodium potassium mixed alkali phosphate glass was selected and the optimal Nd^{3+} concentration for the potential laser emission is investigated.

The Judd–Ofelt [13,14] theory has been applied to interpret the local environment of Nd^{3+} in terms of crystal field symmetry and bond covalency, studying changes of the experimentally fitted Judd–Ofelt parameters. Most of the studies are focused on

* Corresponding author. Tel.: +91 8626 243858; fax: +91 8626 240783.
E-mail address: ratnakaram_yc@yahoo.co.in (Y.C. Ratnakaram).

0925-8388/$ – see front matter © 2009 Elsevier B.V. All rights reserved.
doi:10.1016/j.jallcom.2009.02.033

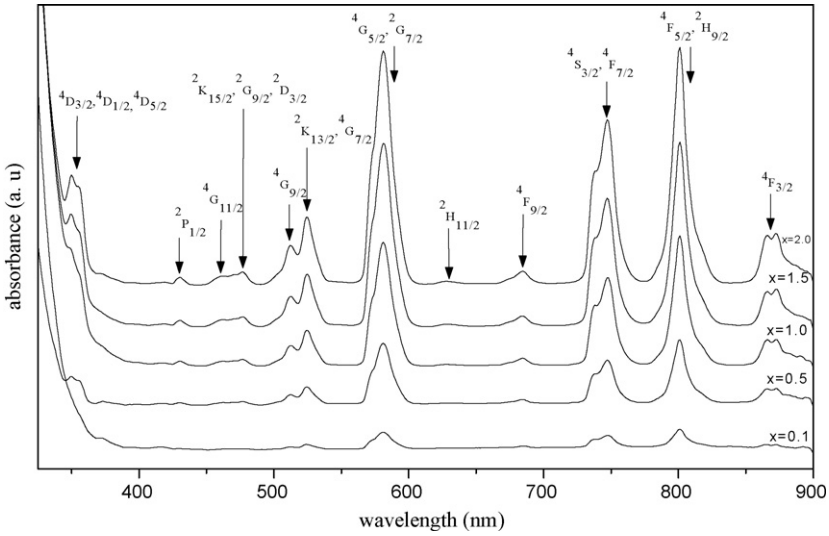

Fig. 1. Optical absorption spectra of different concentrations of Nd^{3+} doped sodium potassium mixed alkali phosphate glass.

systems with relatively low concentrations of REs because, for commercial applications, using high rare earth concentrations is not desirable because of concentration quenching. However, this is not the case for nuclear materials applications, which sometimes require high concentration of rare earths. Recently, effect of Nd^{3+} concentration on the physical and absorption properties of sodium lead borate glasses was reported by Mohan et al. [15]. Spectroscopic and 1.06 μm laser properties of Nd^{3+} doped K–Sr–Al phosphate and fluorophosphate glasses were reported by Upendra Kumar et al. [16]. Chen et al. [17] reported effect of Nd^{3+} on the spectroscopic properties of bismuth borate glasses. Fluorescence and non-radiative properties of Nd^{3+} in novel heavy metal contained fluorophosphate glasses were reported by Choi et al. [18]. Our particular interest in this study is to examine (1) how the Judd–Ofelt parameters are affected by the concentration of REs using Nd as a probing cation and (2) how these parameters are connected with the local structure of Nd–O environments. UV–visible–NIR optical absorption spectra and visible luminescence spectra were measured. Using Judd–Ofelt intensity parameters (Ω_2, Ω_4 and Ω_6) radiative lifetimes, branching ratios and emission cross-sections are reported.

2. Experimental

Sodium potassium mixed alkali phosphate glass doped with different concentrations of Nd_2O_3 was prepared by using high purity analar grade various chemicals, $NH_4H_2PO_4$, Na_2CO_3, K_2CO_3 and Nd_2O_3 in the glass composition $(70-x)P_2O_5$–$15Na_2O$–$15K_2O$–xNd_2O_3 (where x = 0.1, 0.5, 1.0, 1.5 and 2.0 mol%) using melt quenching technique. Among various glass compositions we have prepared, the present glass composition gave good glass for optical studies and therefore we have selected to study the effect of Nd^{3+} concentration on absorption and emission properties in this glass matrix. The appropriate quantities of raw materials are weighed accurately and ground in an agate mortar to produce 10 g each of glass mixture. This mixture was then placed in an electric furnace and melted at 1100 °C for 1 h in a silica crucible. The melt was then quenched between two well-polished preheated brass plates and annealed at 400 °C for 4 h in order to remove mechanical stress. The glass samples of about 1 cm diameter and 0.1–0.15 cm thickness were obtained. The optical quality of all the samples was checked with a microscope and bubble free samples were taken for optical measurements. The thickness of the samples was determined with a micrometer.

The absorption spectra were measured in the 200–1000 nm region using JASCO UV–VIS–NIR spectrophotometer (Model V-570). Fluorescence spectra in the wavelength range 550–750 nm were recorded using PerkinElmer spectrophotometer (Model LS-55) by exciting the sample at 501 nm. PerkinElmer spectrophotometer uses a high-energy Pulsed Xenon source (20 kW for 8 μs duration) for the LS-55 and it has many advantages like minimal photo bleaching of samples, long lived excitation for stability and accuracy, improved low-light detection capability relative to other light sources and wide UV output (to 200 nm), for greater flexibility when selecting wavelengths. All the optical measurements were performed at room temperature. The refractive indices were measured at sodium wavelength using an Abbe refractometer with 1-monobromonaphthalene as an adhesive liquid. The density measurements were done using Archimedes principle using xylene as the immersion liquid.

3. Results and discussion

3.1. Absorption spectra

The room temperature optical absorption spectra of different concentrations of Nd^{3+} doped mixed alkali phosphate glass are shown in Fig. 1. It can be seen that the transition energy levels vary with the concentration and depend on its host matrices indicative of the difference in the degree of bond covalency and the asymmetry of Nd–O local structure among these host matrices. It is observed that the absorption intensity of the observed bands increases with the increase of Nd_2O_3 concentration. Because of the inhomogeneous broadening, the Stark structure is poorly resolved for all the bands but for the excited state, $^4F_{3/2}$ the Stark splitting is clearly observed for all the concentrations. Sometimes adjacent energy levels overlap and appear as single peak in the observed spectra. The broadening of the absorption bands is due to the absence of long-range order in the host producing changes of the micro symmetry around Nd^{3+}. It is also observed that except at 0.5 mol% of Nd_2O_3, the UV absorption edge shifted to a higher wave number side with the increase of Nd_2O_3 concentration.

In the present work, the spectral profile of the absorption peak ($^4D_{3/2}$, $^4D_{1/2}$, $^4D_{5/2}$), nearly at 350 nm varies with the Nd_2O_3 concentration. The rms deviations between the experimental (from the absorption spectra) and calculated (obtained using the method described in Ref. [19]) energies are obtained and these values are very small (±78, ±77, ±78, ±87 and ±93 for 0.1, 0.5, 1.0, 1.5 and

Table 1
Various spectroscopic parameters of Nd^{3+} doped sodium potassium mixed alkali phosphate glasses (all the values except E^1/E^3 and E^2/E^3 are in cm^{-1}) (x in mol%).

S. no.	Parameter	x = 0.1	x = 0.5	x = 1.0	x = 1.5	x = 2.0
1	E^1	4983	4995	5009	4954	4969
2	E^2	23.9	24.3	24.2	24.6	24.6
3	E^3	496.1	495.8	495.9	495.9	496.8
4	ξ_{4f}	871.7	874.3	875.9	890.4	886.4
5	α	3.542	3.403	3.923	4.876	5.209
6	E^1/E^3	10.35	10.35	10.35	10.34	10.34
7	E^2/E^3	0.05	0.06	0.06	0.06	0.06

Table 2
Experimental ($f_{exp} \times 10^6$) and calculated spectral intensities ($f_{cal} \times 10^6$) of certain excited states of Nd^{3+} doped sodium potassium mixed alkali phosphate glass (x in mol%).

S. no.	Energy level	$x = 0.1$		$x = 0.5$		$x = 1.0$		$x = 1.5$		$x = 2.0$	
		f_{exp}	f_{cal}	f_{exp}	f_{cal}	f_{exp}	f_{cal}	f_{exp}	f_{cal}	f_{exp}	f_{cal}
1	$^4F_{3/2}$	1.72	3.61	1.46	2.94	2.42	3.91	2.78	3.74	2.61	3.45
2	$^4F_{5/2}$, $^2H_{9/2}$	16.17	14.81	13.67	12.62	14.66	13.56	13.98	13.20	12.42	11.54
3	$^4F_{7/2}$, $^4S_{3/2}$	15.52	16.67	13.48	14.46	13.10	14.43	13.52	14.16	11.45	12.29
4	$^4F_{9/2}$	1.76	1.26	0.89	1.09	0.92	1.12	1.02	1.09	0.84	0.94
5	$^2H_{11/2}$	0.28	0.34	0.18	0.29	0.24	0.31	0.16	0.29	0.14	0.26
6	$^4G_{5/2}$, $^2G_{7/2}$	32.89	33.03	30.32	30.37	31.6	31.58	30.73	30.69	26.46	26.52
7	$^2K_{13/2}$, $^4G_{7/2}$	9.13	7.81	7.48	6.73	8.29	7.72	7.99	7.45	6.55	6.64
8	$^4G_{9/2}$	4.64	2.7	4.26	2.27	4.69	2.68	3.94	2.59	3.64	2.32
9	$^2K_{15/2}$, $^2G_{9/2}$, $^2D_{3/2}$	1.66	1.93	1.78	1.61	1.63	1.91	1.25	1.84	1.17	1.66
10	$^4G_{11/2}$	1.76	4.18	1.51	0.35	1.66	0.39	1.71	0.38	1.46	0.34
	rms deviation		±1.37		±0.96		±1.02		±0.76		±0.70

2.0 mol% of Nd_2O_3) indicating that full matrix diagonalization procedure leads to a good fit between the observed and calculated energies. The Racah (E^1, E^2, E^3), spin-orbit (ξ_{4f}) and configuration interaction (α) parameters and hydrogenic ratios (E^1/E^3 and E^2/E^3) of different concentrations of Nd_2O_3 are calculated using the procedure explained earlier [19] and are presented in Table 1. The hydrogenic ratios are more or less same for all the concentrations of Nd^{3+} doped mixed alkali phosphate glass indicating that the radial properties of Nd^{3+} ions in different concentrations are not affected.

3.2. Application of Judd–Ofelt theory

Judd–Ofelt theory can describe the radiative properties of rare earth ions in a variety of host materials like glasses and crystals. This theory is well established in the literature and therefore only the relevant equations are employed to analyze our results and are presented here. The experimental spectral intensities (f_{exp}) of the observed absorption bands were measured from the area under the each absorption band using the formula:

$$f_{exp} = 4.318 \times 10^{-9} \int \varepsilon(\nu) d\nu \quad (1)$$

where $\varepsilon(\nu) = OD/cl$ is the molar extinction coefficient at mean energy ν (cm^{-1}), with OD being the optical density, c being the molar concentration of lanthanide ion and l is the optical path length. Using Judd–Ofelt theory [13,14] calculated spectral intensities are obtained. In the present work, in the calculation of electric dipole line strengths, we have used the squared reduced matrix elements reported by Carnall et al. [20] because these values are host invariant. The experimental and calculated spectral intensities (f) of the observed bands of Nd^{3+} and the rms deviations between these two are presented in Table 2 for different concentrations. The rms deviations between the experimental and calculated values are very small, confirming the validity of Judd–Ofelt theory. The spectral intensities of most of the transitions are high for the glasses with $x = 0.1$ mol% of Nd_2O_3 and low for the glasses with $x = 2.0$ mol% of Nd_2O_3 indicating higher and lower crystal field asymmetries in the vicinity of Nd^{3+} ion in these two glass matrices respectively.

Using experimental spectral intensities and the values of squared reduced matrix elements, the best set of Judd–Ofelt intensity parameters (Ω_2, Ω_4 and Ω_6) are obtained applying least squares fit method. These values are presented in Table 3 along with the parameters in other glass hosts. The Ω_2 parameter is sensitive to both asymmetry and covalency at the rare earth sites [21]. In the present work, it is observed that the Ω_2 parameter decreases with the increase of Nd^{3+} concentration indicating decrease in covalency between neodymium cation and oxygen anion with the increase of Nd^{3+} concentration. The Ω_6 parameter followed the same trend as the Ω_2 parameter indicating decrease in the rigidity of the host matrix with the increase of Nd^{3+} concentration. The order of magnitude of Judd–Ofelt intensity parameters for $x = 0.1$, 0.5, 1.0 and 1.5 mol% is $\Omega_4 < \Omega_2 < \Omega_6$ and for $x = 2.0$ mol%, the order is $\Omega_2 < \Omega_4 < \Omega_6$. The Judd–Ofelt parameters obtained in the present work are consistent with the values reported in literature [10] for lithium sodium and lithium potassium mixed alkali borate glasses. From Table 3, it is observed that the magnitude of Ω_2 parameter is larger in mixed alkali phosphate glasses (i.e. in the present work) when compared with the sodium borate, bismuth borate and calcium alumino silicate glasses indicating more covalency. Oomen and van Dongen [22] suggested that it is appropriate to observe the variation of the sum of Judd–Ofelt parameters, $\Sigma\Omega_\lambda$ with the variation of covalency instead of observing only the variation in Ω_2 parameter. In the present work, it is observed that $\Sigma\Omega_\lambda$ value decreases with the increase of Nd^{3+} concentration except at $x = 0.5$ mol%. It is also observed that the sum of Judd–Ofelt intensity parameters, $\Sigma\Omega_\lambda$ decreases with the increase of Nd^{3+} concentration in potassium borate glass. In potassium borate glass, $\Sigma\Omega_\lambda$ value decreases up to $x = 1.5$ mol% and then increased at $x = 2.0$ mol% of Nd_2O_3. For sodium lead borate and calcium alumino silicate glasses, $\Sigma\Omega_\lambda$ increases with the increase of Nd^{3+} concentration. Variation of Ω_2 parameter and $\Sigma\Omega_\lambda$ with Nd^{3+} concentration in the present work is shown in Fig. 2. Ω_λ can also be obtained from

$$\Omega_\lambda = (2t+1)\sum_{s,p} |A_{s,p}|\, \Xi^2(s,\ t)(2s+1)^{-1} \quad t = 2, 4, 6 \quad (2)$$

where $A_{s,p}$ are the crystal field parameters of rank s and are related to the structure around rare earth ions. $\Xi(s, t)$ is related to the host matrix elements between the two radial wave functions of 4f and the admixing levels e.g. 5d, 5g and the energy difference between these levels. It has been suggested by Reisfeld and Jorgensen [23] that Ξ correlates to the nephelauxetic parameter β, which indicates the degree of covalency of the R–O bond.

3.3. Hypersensitive transition

The position and intensity of certain transitions are sensitive to the environment of the rare earth ion. These transitions follow the selection rules $\Delta J \leq 2$, $\Delta L \leq 2$ and $\Delta S = 0$. For Nd^{3+} ion, $^4I_{9/2} \rightarrow {}^4G_{5/2} + {}^2G_{7/2}$ is the hypersensitive transition. In the present work, the spectral intensities of the hypersensitive transition decreases with the increase of Nd^{3+} concentration except small deviation at $x = 0.5$ mol%. It is observed that the intensity of hypersensitive transition shows maximum at $x = 0.1$ mol% and minimum at $x = 2.0$ mol% of Nd_2O_3. This indicates that the nonsymmetric component of electric field acting on Nd^{3+} ion is higher for glass containing 0.1 mol% and lower for 2.0 mol% of Nd_2O_3. It is also observed that the values of Ω_2 parameter are found to be proportional to the intensity of the hypersensitive transition, in accordance with the theory [21]. Further, Krupke [24] pointed out that the

Table 3
Judd–Ofelt intensity parameters ($\Omega_\lambda \times 10^{20}$, $\lambda = 2, 4, 6$) (cm^2) of Nd^{3+} doped in different concentrations (in mol%) in various glass matrices.

S. no.	Glass matrix	Parameter	0.1	0.5	1.0	1.5	2.0
1	Sodium potassium mixed alkali phosphate [present work]	Ω_2	8.03	7.88	6.94	6.83	5.59
		Ω_4	5.73	4.53	6.85	6.50	6.15
		Ω_6	11.31	9.78	9.61	9.44	8.05
		$\Sigma\Omega_\lambda$	25.07	22.19	23.40	22.76	19.79
2	Potassium borate [34]	Ω_2	–	7.19	6.30	4.56	5.56
		Ω_4	–	3.30	3.29	5.34	6.99
		Ω_6	–	3.70	4.24	3.75	5.21
		$\Sigma\Omega_\lambda$	–	14.19	13.83	13.65	17.76
3	Sodium lead borate [15]	Ω_2	–	–	2.58	4.05	3.67
		Ω_4	–	–	2.59	3.38	4.37
		Ω_6	–	–	2.98	4.71	5.50
		$\Sigma\Omega_\lambda$			8.15	12.14	13.64
4	Calcium alumino silicate [35]	Ω_2	–	3.11	3.21	3.20	3.13
		Ω_4	–	4.18	4.07	4.51	4.65
		Ω_6	–	1.92	2.01	1.98	2.06
		$\Sigma\Omega_\lambda$		9.21	9.29	9.69	9.84
5	Bismuth borate [17]	Ω_2	3.71	3.28	3.22	2.70	2.61
		Ω_4	2.59	3.88	3.84	4.10	3.86
		Ω_6	4.24	4.24	4.33	4.47	4.24
		$\Sigma\Omega_\lambda$	10.54	11.40	11.39	11.27	10.71

intensity of the hypersensitive transition, $^4I_{9/2} \rightarrow {}^4G_{5/2} + {}^2G_{7/2}$ is determined mainly by Ω_2 parameter. The Stark splitting due to the crystal field splits this transition into two peaks in the absorption spectra. In the present work, the Stark splitting decreases with the increase of Nd_2O_3 concentration and the splitting is hidden by the inhomogeneous broadening at higher concentrations. The shift in the peak wavelength of the hypersensitive transition towards longer wavelengths indicates increase in covalency of RE–O bond (because of nephelauxetic effect [23]). In the present work, it is observed that there is no shift in the position of the peak wavelength of the hypersensitive transition for different concentrations of Nd_2O_3 except small increase at $x = 0.1$–0.5 mol% (580.0–580.7 nm).

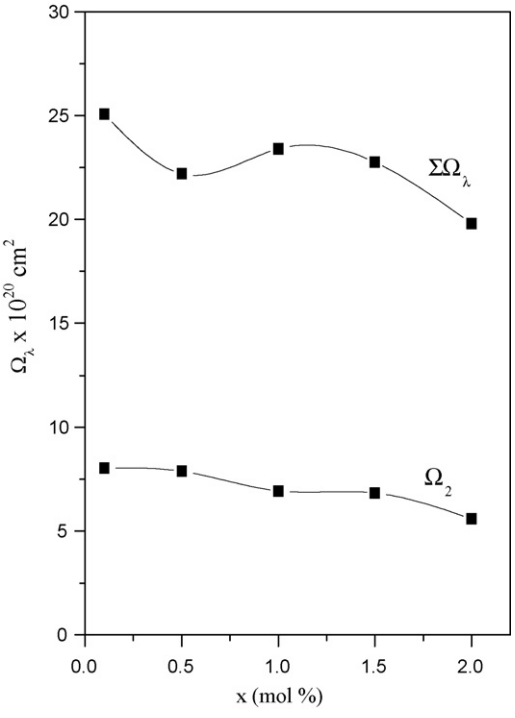

Fig. 2. Variation of Ω_2 parameter and $\Sigma\Omega_\lambda$ with Nd^{3+} concentration in sodium potassium mixed alkali phosphate glass.

The Ω_2 parameter slightly decreased (8.03×10^{-20} to 7.88×10^{-20}) at this composition indicating that the structural changes, if any are not influencing much the covalency of Nd–O bond. The spectral profile of the hypersensitive transition, $^4I_{9/2} \rightarrow {}^4G_{5/2} + {}^2G_{7/2}$ is same for all the concentrations.

3.4. Radiative properties

Using Judd–Ofelt intensity parameters, Ω_2, Ω_4 and Ω_6, electric dipole line strengths (S_{ed}), radiative transition probabilities (A_{rad}), branching ratios (β_R) and integrated absorption cross-sections (Σ) of different transitions of excited states are calculated using standard formulae [23]. In the present work, total radiative transition probabilities and radiative lifetimes are calculated for the excited states, $^4G_{9/2}$, $^4G_{7/2}$, $^4G_{5/2}$, $^2H_{11/2}$, $^4F_{9/2}$, $^4F_{5/2}$ and $^4F_{3/2}$ of Nd^{3+} and are presented in Table 4. It is observed that the total radiative transition probabilities of all the excited states are decreasing with the increase of Nd^{3+} concentration except small deviation at $x = 0.5$ mol%. It is also observed that total radiative transition probabilities are decreasing with the decrease of covalency (Ω_2 parameter) of the Nd–O bond except at $x = 0.5$ mol%. This lower radiative transition probability at $x = 0.5$ mol% could be correlated to the lower Ω_4 parameter attributing lower rigidity of the host matrix. The radiative lifetime (τ_R) represents an effective average over site–site variations in the local Nd^{3+} environment. It is observed that the estimated radiative lifetimes of all the excited states are lower at $x = 0.1$ mol% and higher at $x = 2.0$ mol%. At low Nd^{3+} concentration (<0.5 mol%), the radiative lifetimes increase with the increase of Nd^{3+} concentration from 0.1 to 0.5 mol% of Nd_2O_3. It is known that when a small amount of Nd^{3+} ions is doped into glass, some changes occur in their network structure [25]. Therefore the influence of concentration quenching is weak at low Nd^{3+} concentrations; changes of the environment around Nd^{3+} ions may be the reason for the changes of the lifetimes with the Nd^{3+} concentration. At higher Nd^{3+} concentrations (>0.5 mol%), the concentration quenching process becomes predominant and the fluorescence lifetimes decreases with increasing Nd^{3+} concentration from 0.5 to 1.5 mol%. In other words, clustering of Nd^{3+} ions proceed up to 0.5 mol% of Nd_2O_3 and at >0.5 mol%, Nd^{3+} ions are in the poorly dispersed state. At 2.0 mol% of Nd_2O_3, radiative lifetimes are slightly increased. Similar trend has been observed in the case of fluorophosphate glasses [18]. Variation of A_T parameter with Nd^{3+} concentration is shown in Fig. 3 The radiative lifetimes obtained in

Table 4
Total radiative transition probabilities (A_T) (s^{-1}) and radiative lifetimes (τ_R) (μs) of certain excited states of Nd^{3+} doped sodium potassium mixed alkali phosphate glasses (x in mol%).

S. no.	Excited state	$x=0.1$		$x=0.5$		$x=1.0$		$x=1.5$		$x=2.0$	
		A_T	τ_R	A_T	τ_R	A_T	τ_R	A_T	τ_R	A_T	τ_R
1	$^4G_{9/2}$	21,977	46	19,630	51	21,252	47	20,625	49	17,905	56
2	$^4G_{7/2}$	20,350	49	18,567	54	19,486	51	18,818	53	16,349	61
3	$^4G_{5/2}$	30,988	32	28,152	36	29,605	34	28,762	35	24,889	40
4	$^2H_{11/2}$	646	549	589	698	635	574	613	629	532	880
5	$^4{}_{/2}$	6,799	147	5,766	173	6,146	162	6,000	167	5,146	194
6	$^4F_{5/2}$	8,200	122	6,907	145	7,689	130	7,471	134	6,558	153
7	$^4F_{3/2}$	6,321	158	5,288	189	6,016	166	5,833	171	5,166	194

the present work are comparable to the radiative lifetimes of Nd^{3+} in sodium potassium mixed alkali borate glasses at $x=2.0$ mol% [21].

The branching ratios (β_R) and integrated absorption cross-sections (Σ) are evaluated for different transitions of Nd^{3+} for all the concentrations. These values, which are higher in their magnitudes for certain transitions are collected in Table 5. It is observed that the branching ratio values of most of the transitions are higher at $x=0.5$ mol% and lower at $x=2.0$ mol%. Among various transitions, the transition, $^4G_{5/2} \rightarrow {}^4I_{9/2}$ has higher branching ratio value. The Ω_2 parameter becomes independent in characterizing the fluorescent properties of $^4F_{3/2} \rightarrow {}^4I_J$ ($J=9/2, 11/2, 13/2$) transitions because the values of $||U^2||^2$ are zero for all these transitions. Hence the radiative properties depend on Ω_4 and Ω_6 parameters because of the triangle rule $|J-J'| \leq \lambda \leq |J+J'|$ [26]. In the present work, the branching ratios of the two emission transitions: $^4F_{3/2} \rightarrow {}^4I_{9/2}$ and $^4G_{5/2} \rightarrow {}^4I_{9/2}$ are in the range 0.667–0.723 and 0.779–0.817 respectively for different concentrations. The branching ratio of the transition, $^4F_{3/2} \rightarrow {}^4I_{9/2}$ is more at 0.1 mol% of Nd_2O_3 (0.723) and for $^4G_{5/2} \rightarrow {}^4I_{9/2}$ transition, it is more at 0.5 mol% of Nd_2O_3 (0.817). Therefore the efficiency for $^4F_{3/2} \rightarrow {}^4I_{9/2}$ transition is more at 0.1 mol% and the efficiency for $^4G_{5/2} \rightarrow {}^4I_{9/2}$ transition is more at 0.5 mol% of Nd_2O_3.

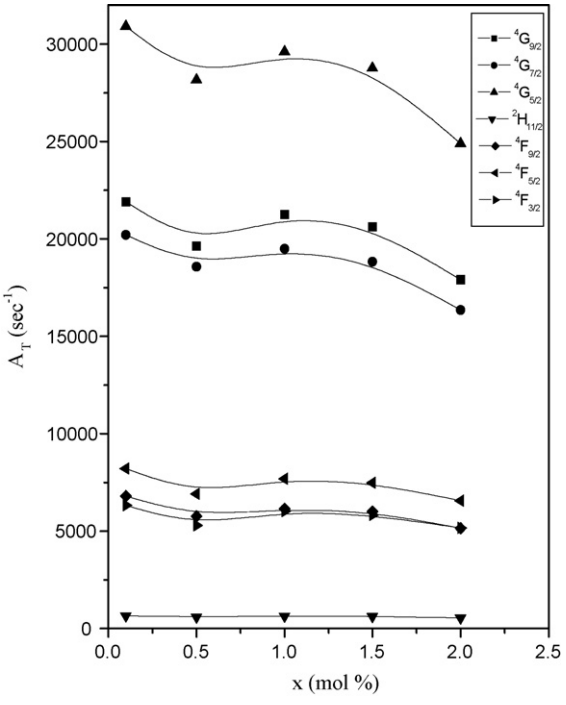

Fig. 3. Variation of total radiative transition probability (A_T) with Nd^{3+} concentration in sodium potassium mixed alkali phosphate glass.

3.5. Photoluminescence spectra

The luminescence spectra of different concentrations of Nd_2O_3 doped sodium potassium mixed alkali phosphate glass recorded in the wavelength region 570–740 nm under the excitation wavelength of 501 nm are shown in Fig. 4. Due to lack of experimental facilities, the properties of the emission transition, $^4F_{3/2} \rightarrow {}^4I_{11/2}$ of Nd^{3+} have not studied though it is one of the important transitions of Nd^{3+} ion. In the present work, two emission bands corresponding to the transitions, $^4G_{7/2} \rightarrow {}^4I_{13/2}$ and $^4G_{7/2} \rightarrow {}^4I_{11/2}$ appear nearly at 660 and 600 nm respectively. From the spectra, it is observed that concentration effect is evident in the line shape evolution [27]. Among the five Nd^{3+} concentrations, the maximum intensity was observed for 0.1 mol% of Nd_2O_3. From the analysis of the emission spectra, it can be seen that the shape of the emission bands is same for all the concentrations of Nd_2O_3. This invariance indicates that the ion–ion interaction between Nd^{3+} sites is strong as observed by Brecher et al. [28], Riseberg [29] and Kalisky et al. [30]. At larger Nd^{3+} concentrations, the intensity of fluorescence decreases due to the onset of spectral diffusion [29]. The coupling between the ions is source of diffusion. In the present work, emission intensity is very small at 0.5 and 1.5 mol% of Nd_2O_3 when compared with 0.1, 1.0 and 2.0 mol% of Nd_2O_3 and also small splitting is observed at these two concentrations. The bandwidths of I_{peak} (660 nm) and I_{peak} (600 nm) are constant for all the concentrations, but the ratio of the peak intensities $r = I_{peak}$ (600 nm)/I_{peak} (660 nm) can be fitted to a parabolic function (Fig. 5) corresponding to the general formula:

$$r(c) = 0.1695c^2 - 0.3861c + 0.7974$$

where c represents Nd_2O_3 concentration. In addition, I_{peak} (660 nm) and I_{peak} (600 nm) correspond to the peak intensities of the emissions resulting from the transitions, $^4G_{7/2} \rightarrow {}^4I_{13/2}$ and $^4G_{7/2} \rightarrow {}^4I_{11/2}$ respectively.

As shown in Fig. 5, the minimum on the graph of $r(c)$ is located between 0.5 and 1.5 compositions. The neodymium concentration at this minimum is 3.25 wt% (c_m). When c increases from zero to c_m, the transition $^4G_{7/2} \rightarrow {}^4I_{13/2}$ is more favorable than $^4G_{7/2} \rightarrow {}^4I_{11/2}$ transition. Consequently, the fluorescence related to the latter transition diminishes in comparison with that of the former one, resulting in a decrease of $r(c)$. For $c > c_m$, the intensity of the emission corresponding to the transition, $^4G_{7/2} \rightarrow {}^4I_{11/2}$ peaking at 600 nm is increased with regard to I_{peak} (660). This increase probably be explained by a competition between the two transitions, $^4G_{7/2} \rightarrow {}^4I_{11/2}$ and $^4G_{7/2} \rightarrow {}^4I_{13/2}$, where the latter is favorable. Consequently, the ratio $r(c)$ has increased since the intensity I_{peak} (600 nm) diminishes. This increase is compatible with the presence of pairs of Nd^{3+}, which promotes the $^4G_{7/2}$ de-excitation via $^4G_{7/2} \rightarrow {}^4I_{13/2}$ preferably to $^4G_{7/2} \rightarrow {}^4I_{11/2}$ channel. Judd–Ofelt theory can successfully account for the observed stimulated emission cross-sections. The peak stimulated emission cross-sections (σ_p) of

Table 5
Branching ratios (β) and integrated absorption cross-sections ($\Sigma \times 10^{18}$) (cm) of certain transitions of Nd^{3+} doped sodium potassium mixed alkali borate glasses (x in mol%).

S. no.	Transition	$x = 0.1$		$x = 0.5$		$x = 1.0$		$x = 1.5$		$x = 2.0$	
		β	Σ	β	Σ	β	Σ	β	Σ	β	Σ
1	$^4G_{9/2} \rightarrow {}^4I_{13/2}$	0.492	22.2	0.512	20.8	0.474	20.8	0.477	20.3	0.465	17.3
2	$^4G_{7/2} \rightarrow {}^4I_{11/2}$	0.547	18.6	0.572	17.9	0.511	16.7	0.515	16.3	0.496	13.7
3	$^4G_{5/2} \rightarrow {}^4I_{9/2}$	0.802	40.9	0.817	38.1	0.786	38.5	0.788	37.5	0.779	32.2
4	$^2H_{11/2} \rightarrow {}^4I_{15/2}$	0.472	1.6	0.483	1.5	0.471	1.6	0.471	1.5	0.462	1.3
5	$^4F_{3/2} \rightarrow {}^4I_{9/2}$	0.723	17.4	0.667	14.7	0.667	16.2	0.667	15.7	0.668	13.8
6	$^4F_{3/2} \rightarrow {}^4I_{11/2}$	0.542	18.5	0.549	15.7	0.509	16.6	0.513	16.3	0.502	14.1

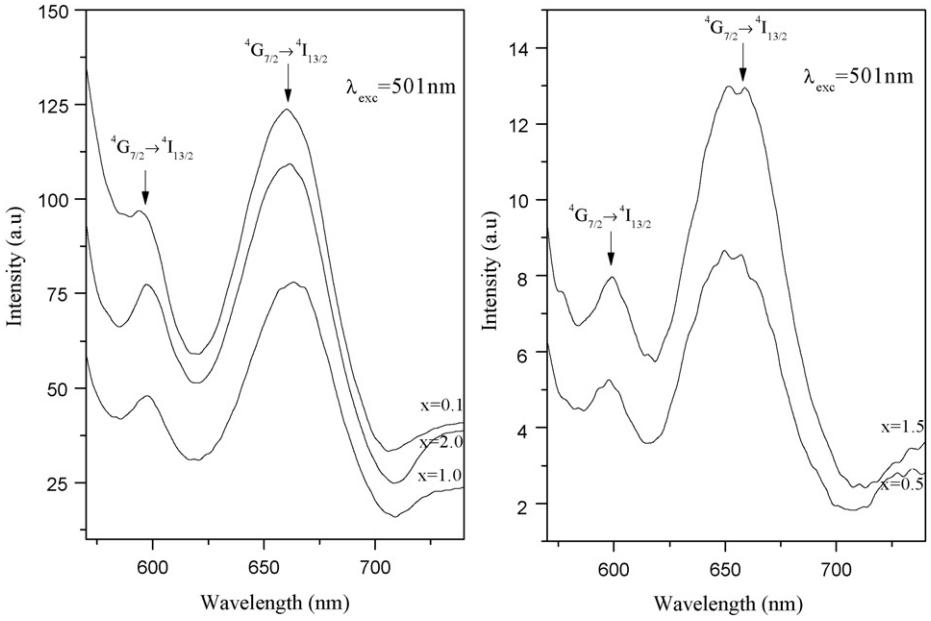

Fig. 4. Fluorescence spectra of different concentrations of Nd^{3+} doped sodium potassium mixed alkali phosphate glass.

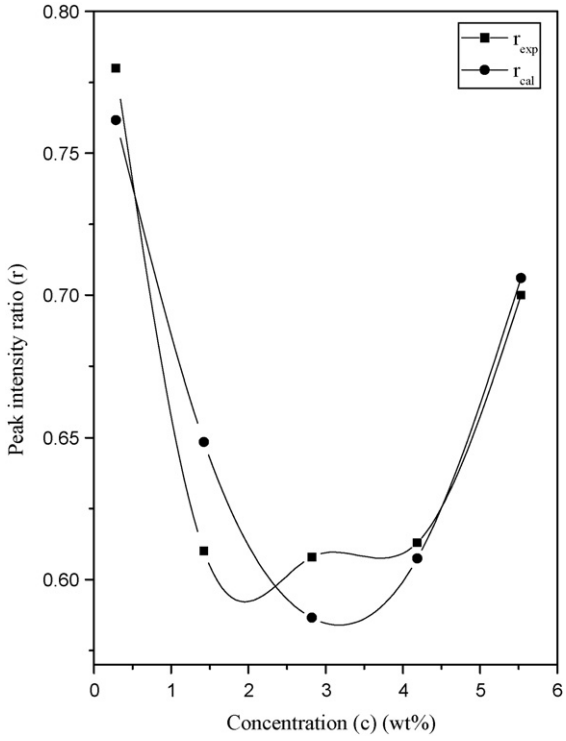

Fig. 5. Variation of peak intensity ratio (r) with Nd^{3+} concentration in sodium potassium mixed alkali phosphate glass.

the above two transitions are calculated using the formula [31]:

$$\sigma_p = \frac{\lambda_p^4}{8\pi c n^2 \Delta\lambda_{eff}} A(aJ, bJ') \quad (3)$$

where λ_p is the peak wavelength, $\Delta\lambda_{eff}$ is the effective linewidth of the emission band and $A(aJ, bJ')$ is the radiative transition probability. From Eq. (3), it is observed that σ_p depends on the intensity parameters Ω_λ, the bandwidth $\Delta\lambda_{eff}$ and the refractive index n. Both Ω_λ and $\Delta\lambda_{eff}$ are affected by compositional changes. Table 6 gives peak wavelengths (λ_p), radiative transition probabilities (A), effective linewidths ($\Delta\lambda_{eff}$) and peak emission cross-sections (σ_p) of the two transitions, $^4G_{7/2} \rightarrow {}^4I_{13/2}$ and $^4G_{7/2} \rightarrow {}^4I_{11/2}$ of different concentrations of Nd^{3+} in sodium potassium mixed alkali phosphate glass. It is observed that peak emission cross-section values are higher for 0.1 mol% of Nd_2O_3 and lower for 2.0 mol% of Nd_2O_3 among all the concentrations. The emission band, $^4G_{7/2} \rightarrow {}^4I_{11/2}$ has large stimulated cross-section, which is an attractive feature for low threshold and high gain applications. Hence the emission band $^4G_{7/2} \rightarrow {}^4I_{11/2}$ at $x = 0.1$ mol% has been identified as a potential lasing transition. Variation of peak emission cross-section (σ_p) with Nd^{3+} concentration is shown in Fig. 6.

3.6. Optical band gaps

The absorption edge of nonmetallic materials gives a measure of the band strength or energy gap. Davis and Mott [32] obtained optical band gaps (E_{opt}) for both direct and indirect transitions using

Table 6
Certain fluorescence properties of different concentrations of Nd^{3+} doped sodium potassium mixed alkali phosphate glasses.

S. no.		$^4G_{7/2} \rightarrow {}^4I_{11/2}$				$^4G_{7/2} \rightarrow {}^4I_{13/2}$			
		λ_p (nm)	A (s^{-1})	$\Delta\lambda_{eff}$ (cm^{-1})	σ_p (10^{-19})	λ_p (nm)	A (s^{-1})	$\Delta\lambda_{eff}$ (cm^{-1})	σ_p (10^{-20})
1	$x = 0.1$	595	20,211	58.7	6.01	661	20,211	577.4	7.54
2	$x = 0.5$	598	18,567	78.9	4.14	657	18,567	679.6	5.81
3	$x = 1.0$	597	19,486	95.9	3.57	663	19,486	664.4	6.36
4	$x = 1.5$	599	18,818	90.1	3.69	659	18,818	672.5	5.99
5	$x = 2.0$	597	16,349	98.5	2.92	661	16,349	613.2	5.75

the formula:

$$\alpha(\omega) = \frac{B(\hbar\omega - E_{opt})^n}{\hbar\omega} \quad (4)$$

where $\alpha(\omega)$ is the absorption coefficient, B is a constant, $\hbar\omega$ is the photon energy of the incident radiation, E_{opt} is the optical band gap and n an index which can assume values 1, 2, 3, 1/2 or 3/2 depending on the nature of the inter-band electronic transitions. The above equation with $n = 2$ agrees well for chalcogenide and oxide glasses [33]. For direct transitions $n = 1/2$ and for indirect transitions $n = 2$. Optical band gap values are obtained both for indirect and direct transitions of Nd^{3+} doped mixed alkali phosphate glass from the variation of $(\alpha\hbar\omega)^{1/2}$ with $\hbar\omega$ and from the variation of $(\alpha\hbar\omega)^2$ with $\hbar\omega$ graphs respectively. The respective values of E_{opt} are obtained by extrapolating to $(\alpha\hbar\omega)^2 = 0$ for direct transitions and $(\alpha\hbar\omega)^{1/2} = 0$ for indirect transitions. It is observed that the optical band gaps for indirect transitions are 3.372, 3.585, 3.587, 3.593 and 3.594 eV and for direct transitions these values are 3.369, 3.586, 3.587, 3.592 and 3.595 eV for 0.1, 0.5, 1.0, 1.5 and 2.0 mol% respectively. From the above data it is said that the optical band gaps for both indirect and direct transitions are smaller at 0.1 mol% of Nd_2O_3 and larger at 2.0 mol% of Nd_2O_3. The optical band gaps for both indirect and direct transitions increase with the increase of Nd^{3+} concentration.

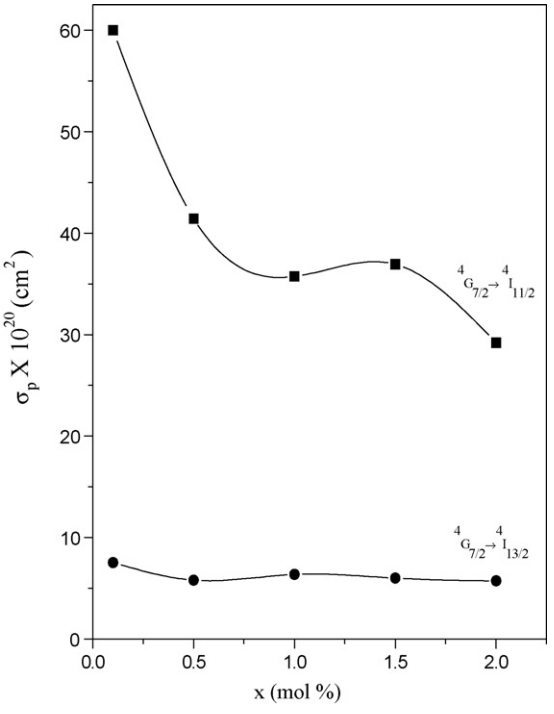

Fig. 6. Variation of peak emission cross-section (σ_p) with Nd^{3+} concentration in mixed alkali phosphate glass.

4. Conclusions

Ω_2 parameter decreased with the increase of Nd^{3+} concentration indicating decrease in covalency of Nd–O bond in this sodium potassium phosphate glass. The sum of Judd–Ofelt intensity parameters ($\Sigma\Omega_\lambda$) also decreased with the increase of Nd^{3+} concentration (except at $x = 0.5$ mol%), which is attributed to the nature of covalency of Nd–O bond. The spectral profiles of the hypersensitive transition are same for different concentrations of Nd^{3+}. There is a decrease in the intensity of hypersensitive transition with an increase of x (except at $x = 0.5$ mol%), indicating lower asymmetry at higher Nd^{3+} concentrations. No peak splitting of the hypersensitive transition is observed for any of the Nd^{3+} concentration studied. From the variation of peak wavelength of the hypersensitive transition and Ω_2 parameter, it is concluded that the influence of structural changes on covalency of Nd–O bond is less. The total radiative transition probabilities of all the excited states of Nd^{3+} are decreased with the increase of Nd^{3+} concentration (except at $x = 0.5$ mol%). The radiative lifetimes of all the excited states are low at $x = 0.1$ mol% and high at $x = 2.0$ mol%. The branching ratios are higher at $x = 0.5$ mol% among different concentrations. It is observed that the transition, $^4G_{5/2} \rightarrow {}^4I_{9/2}$ at $x = 0.5$ mol% is more suitable for laser excitation. Peak stimulated emission cross-sections are calculated for the two emission transitions, $^4G_{7/2} \rightarrow {}^4I_{13/2}$ and $^4G_{7/2} \rightarrow {}^4I_{11/2}$ of Nd^{3+} and these values are higher for 0.1 mol% of Nd_2O_3 and lower for 2.0 mol% of Nd_2O_3. From the peak stimulated emission cross-sections, it is identified that the emission band, $^4G_{7/2} \rightarrow {}^4I_{11/2}$ at $x = 0.1$ mol% may be a potential lasing transition. The optical band gaps for both indirect and direct transitions increased with the increase of Nd^{3+} concentration.

Acknowledgements

The author Prof. Y.C. Ratnakaram expresses his thanks to the University Grants Commission, New Delhi for providing financial assistance in the form of a major research scheme.

References

[1] M. Dejneka, B. Samson, Mater. Res. Soc. Bull. 24 (1999) 39.
[2] M.J. Weber, J. Non-Cryst. Solids 42 (1980) 189.
[3] J.A. Wilder, J. Non-Cryst. Solids 38/39 (1980) 879.
[4] R.K. Brow, D.R. Tallant, J.J. Hudgens, S.W. Martin, A.D. Irvin, J. Non-Cryst. Solids 177 (1994) 221.
[5] D.E. Day, J. Non-Cryst. Solids 21 (1976) 343.
[6] A.H. Dietzel, Phys. Chem. Glasses 24 (1983) 172.
[7] M. Ingram, Glastech. Ber. 67 (1994) 151.
[8] B. Roling, M. Ingram, J. Non-Cryst. Solids 265 (2000) 1.
[9] P.F. Green, D. Sidebottom, R.K. Brow, J. Non-Cryst. Solids 172–174 (1994) 1353.
[10] Y.C. Ratnakaram, A. Vijayakumar, D. Tirupathi Naidu, R.P.S. Chakradhar, K.P. Ramesh, J. Lumin. 110 (2004) 65.
[11] Y.C. Ratnakaram, A. Vijayakumar, R.P.S. Chakradhar, J. Lumin. 118 (2006) 227–237.
[12] Y.C. Ratnakaram, D. Tirupathi Naidu, A. Vijayakumar, J.L. Rao, J. Phys. C: Condens. Matter 16 (2004) 3779.
[13] B.R. Judd, Phys. Rev. 127 (1962) 750.
[14] G.S. Ofelt, J. Chem. Phys. 37 (1962) 511.
[15] S. Mohan, K.S. Thind, G. Sharma, Brazilian J. Phys. 37 (2007) 4.
[16] K. Upendra Kumar, P. Babu, K.H. Jang, H.J. Seo, C.K. Jayasankar, A.S. Joshi, J. Alloys Compd. 458 (2008) 509.

[17] Y. Chen, Y. Huang, M. Huang, R. Chen, Z. Luo, J. Am. Ceram. Soc. 88 (1) (2005) 19–23.
[18] J.H. Choi, A. Margaryan, A. Margaryan, F.G. Shi, W. Van Der Veer, Adv. OptoElectron. 2007 (2007) (Article ID 39892).
[19] E.Y. Wong, J. Chem. Phys. 35 (1961) 544.
[20] W.T. Carnall, H. Cross White, H.M. Cross White, Energy level structure and transition probabilities in the spectra of the trivalent lanthanides in LaF_3, Argonne National Laboratory Report, 1977.
[21] R. Reisfeld, Struct. Bond. 22 (1975) 123.
[22] E.W.J.L. Oomen, A.M.A. Van Dongen, J. Non-Cryst. Solids 111 (1989) 205.
[23] R. Reisfeld, C.K. Jorgensen, Handbook on the Physics and Chemistry of Rare Earths, vol. 9, North-Holland, Amsterdam, 1998 (Chapter 58), p. 1, 187.
[24] W.F. Krupke, Phys. Rev. 145 (1966) 325.
[25] J.A. Sampaio, M.L. Baesso, S. Gama, A.A. Coelho, J.A. Eiras, I.A. Santos, J. Non-Cryst. Solids 304 (1–3) (2002) 293.
[26] Y.C. Ratnakaram, N. Sudharani, J. Phys. Chem. Solids 59 (1998) 215.
[27] B. Viana, A.M. Lejus, D. Saber, N. Duxin, D. Vivein, Opt. Mater. 3 (1994) 307.
[28] C. Brecher, L.A. Riseberg, M.J. Weber, J. Lumin. 18 & 19 (1978) 651.
[29] L.A. Riseberg, Phys. Rev. A 7 (1973) 671.
[30] Y. Kalisky, R. Reisfeld, Y. Haas, Chem. Phys. Lett. 61 (1976) 1.
[31] M. Yamane, Y. Asahara, Glasses for Photonics, Cambridge University Press, Cambridge, 2000.
[32] F.A. Davis, N.F. Mott, Philos. Mag. 22 (1970) 903.
[33] G.R. Moridi, C.A. Hogarth, in: W.E. Spear (Ed.), Proceedings of the Seventh International Conference on Amorphous and Liquid Semiconductors, 1997, p. 688.
[34] Y.C. Ratnakaram, Md. Abdul Altaf, R.P.S. Chakradhar, J.L. Rao, J. Ramakrishna, Phys. Stat. Sol. B 236 (1) (2003) 200–208.
[35] E. Pecoraro, J.A. Sampaio, L.A.O. Nunes, S. Gama, M.L. Baesso, J. Non-Cryst. Solids 277 (2000) 73–81.